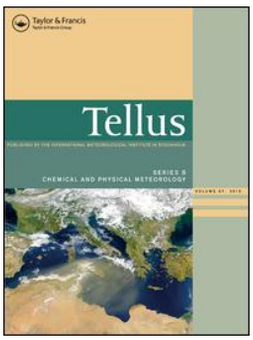

Tellus B: Chemical and Physical Meteorology

ISSN: (Print) 1600-0889 (Online) Journal homepage: http://www.tandfonline.com/loi/zelb20

Modelling the long-range transport of ^{222}Rn to subantarctic and antarctic areas

Martin Heimann, Patrick Monfray & Georges Polian

To cite this article: Martin Heimann, Patrick Monfray & Georges Polian (1990) Modelling the long-range transport of ^{222}Rn to subantarctic and antarctic areas, Tellus B: Chemical and Physical Meteorology, 42:1, 83-99, DOI: 10.3402/tellusb.v42i1.15194

To link to this article: https://doi.org/10.3402/tellusb.v42i1.15194

Published online: 18 Jan 2017.

Tellus (1990), *42B*, 83–99

Modeling the long-range transport of ^{222}Rn to subantarctic and antarctic areas

By MARTIN HEIMANN†, PATRICK MONFRAY†‡ and GEORGES POLIAN‡,
†*Max-Planck-Institut für Meteorologie, Bundesstrasse 55, D-2000 Hamburg 13, FRG;*
‡*Centre des Faibles Radioactivités, CNRS, F-91198 Gif-sur-Yvette Cedex, France*

(Manuscript received 30 March 1989; in final form 8 August 1989)

ABSTRACT

The long-range advection of ^{222}Rn over the Indian Ocean has been studied using a three-dimensional coarse-grid (8° × 10°) transport model of the global troposphere based on the meteorological fields of the GWE period (December 1978–November 1979). A uniform continental source of ^{222}Rn and a weak, wind-speed dependent oceanic source of ^{222}Rn has been prescribed in the simulations. Model predictions are compared to observations of the ^{222}Rn concentration at three Indian Ocean islands and one station located at the Antarctic coast. The advection of continental ^{222}Rn to these observing sites, each being several thousand kilometers away from major landmasses, requires several days and provides a unique opportunity for the validation of the transport model on time scales ranging from a few days to the seasonal cycle induced by seasonally changing transport patterns. The model is able to simulate several features of the time series observed in the Indian Ocean; however, it fails to correctly predict the seasonal cycle and the short-term concentration variations at the Antarctic coast.

1. Introduction

The radioactive noble gas Radon-222 (^{222}Rn) constitutes a unique tracer of atmospheric transport processes. It is chemically inert and is removed only by radioactive decay ($\tau_{1/2} = 3.8$ d). Its primary source is rather uniformly distributed over the continents where it emanates out of the soil as a member of the natural radioactive decay chain of Uranium-238 (Lambert et al., 1982). The ocean represents a secondary source of atmospheric ^{222}Rn, which is, however, two to three orders of magnitude smaller than the continental ^{222}Rn source. Because of its relatively short lifetime large vertical concentration gradients exist over the continents which may be analyzed in terms of vertical mixing, and in particular with respect to air mass exchanges between the planetary boundary layer and the free troposphere (Liu et al., 1984; Dörr and Münnich, 1987). Furthermore, the strong contrast in source strength between continents and the ocean make ^{222}Rn an ideal marker of continental air masses (Dörr et al., 1983; Polian et al., 1986).

Because of its simple properties, the temporal and spatial distribution of ^{222}Rn in the troposphere is straightforward to simulate by means of atmospheric transport models. Such simulations serve at least three purposes:

(1) The comparison between simulation and observation provides a powerful test of the performance of such transport models.

(2) Because of the simple source-sink configuration of this gas, the simulation provides an intuitive visualization of the complex transport characteristics as far as represented in the model.

(3) The overall transport characteristics of different models may be readily compared by examination of their predicted ^{222}Rn concentration fields.

Only recently several model simulation studies of ^{222}Rn have been published. Most extensively, Brost and Chatfield (1989) investigate the long range transport of ^{222}Rn by means of a high

resolution (190 km by 190 km) tracer model covering one third of the Northern Hemisphere including the North American continent and the North Atlantic ocean. In particular, these authors evaluate the sensitivity of the model predicted concentrations with respect to different model formulations of subgrid scale vertical transport in clouds and numerical advection algorithms. Despite the limited amount of ^{222}Rn observations available they are able to discriminate between various model versions based on the agreement between model simulation and data.

Further modeling studies of atmospheric ^{222}Rn are included in the present volume (see the contributions by Balkanski and Jacob; Feichter and Crutzen; Jacob and Prather; this issue).

In this paper, we present the results of an exploratory study, in which we investigated the performance of a coarse-grid three-dimensional transport model of the global troposphere in simulating the long range transport of ^{222}Rn from the southern hemisphere continents to subantarctic and antarctic areas in the Indian Ocean. Thereby, we focus on the Indian Ocean area because the unique set of measurements obtained by the Centre des Faibles Radioactivités (Gif-sur-Yvette, France) (Polian et al., 1986), on three remote islands and on the Antarctic coast permit an in depth comparison between model prediction and data. Furthermore, the Indian Ocean represents an ideal test area as continental sources are far away from the observing sites, hence continental air masses may be traced over several 1000 km.

The present study parallels in several ways the work by Balkanski and Jacob (1990) who investigate the advection of ^{222}Rn enriched air from the African continent to the Indian Ocean by means of a three-dimensional chemical tracer model based on the meteorological fields of the Goddard Institute of Space Studies (GISS) general circulation climate model (Hansen et al., 1983).

The simulations described in this article were performed by means of a transport model driven by observed wind fields as analyzed in the assimilation system of the European Center for Medium Range Weather Forecast (ECMWF). This permits a direct comparison between simulation and data obtained for the same time period as the meteorology of the transport model. However, compared to the study by Balkanski and Jacob (1990), the present model results were obtained using a coarser resolution (a factor of two in both horizontal directions) and a less sophisticated numerical advection scheme.

In the following sections we will describe briefly the transport model, the simulation experiments and the observational data. Afterwards we will discuss the simulation results in comparison with the data. Thereby we also investigate briefly the rôle of the oceanic contribution of ^{222}Rn to the atmospheric concentration signal at the monitoring locations.

2. The transport model

All the simulations described in this paper have been carried out with a coarse-grid three-dimensional atmospheric transport model. Such a model essentially consists of three components: the advection fields, the parameterization of subgridscale transport and the model code which includes the numerical procedures to solve the transport equation for a tracer.

The model structure and the numerical code of the present model originally have been developed at GISS (Russel and Lerner, 1981). The model has a horizontal resolution of approximately 8° latitude by 10° longitude and 9 layers in the vertical dimension. Sigma coordinates are used in the vertical direction. Different versions of the model have been used in the past to simulate fairly successfully the global scale dispersal of gaseous atmospheric tracers with moderate and long lifetimes, such as CO_2 (Fung et al., 1983; Heimann et al., 1986; Heimann and Keeling, 1989), halocarbons (Prather et al., 1987) and Krypton-85 (Jacob et al., 1987).

The numerical scheme used in calculating advective transport has been developed by Russel and Lerner (1981). This so-called "slopes scheme" solves the tracer transport equation in flux form on a regular grid. In addition to the tracer mass it also uses and calculates the time evolution of the three components of the spatial gradient of tracer mass. The basic computational time step used in the model runs was set to 4 h. It is further subdivided by a factor of two in meridional and a factor of four in zonal direction in order to accommodate the typical size of the wind velocity vectors.

Advective transport in the present version of the transport model is based on wind fields which were obtained during the Global Weather Experiment (GWE) (December 1978–November 1979). Geopotential and horizontal components of the wind velocity were available on a global grid with horizontal resolution of 1.875° on 15 vertical pressure levels and a time resolution of 12 h. These data have been analyzed by the four-dimensional assimilation system of the ECMWF (ECMWF-level IIIb data, Bengtsson et al., 1982). From these data horizontal mass fluxes crossing the border surfaces of the transport model gridboxes were calculated using linear interpolation and integration formulae. The vertical massfluxes were subsequently determined from the continuity of air mass.

The mass fluxes thus established did not entirely conserve mass, in that the vertically integrated divergence of air mass did not match the change in surface pressure for 12 h as recorded in the analyses. Typically, we detected a root mean square vertically integrated residual mass flux divergence of 4% of the vertically integrated air mass for 12 h. In order to achieve continuity of mass we introduced a two-dimensional correction mass flux, whose divergence matched the vertically integrated mass deficit as deduced from the uncorrected mass flux fields. This correction flux was specified as the gradient of a potential which itself was found by solving the resulting Poisson equation. Finally, the obtained correction mass flux was distributed uniformly in the vertical dimension. Details of the data-processing have been described elsewhere (Heimann and Keeling, 1989).

The parameterization of subgrid scale vertical convection is based on a standard climate run of the GISS general circulation model (Hansen et al., 1983) and has been described in detail by Prather et al. (1987). In the present model simulations, this parameterization is prescribed at every grid column and kept constant during each simulated month of the year. The use of a subgrid scale parameterization from a particular run of a climate GCM in conjunction with the GWE wind fields is not entirely consistent. Preferrably subgrid scale vertical transport processes should have been deduced from the GWE fields themselves by means of a submodel for convection, which, however, was not available to us at the time of this study. This constitutes a major limitation of the present model experiments, since vertical subgrid scale transport is the dominant vertical transport mechanism between the lowermost model layers (representing the planetary boundary layer) and the free troposphere above. Indeed we find that over the continents over 90% of the vertical transport of ^{222}Rn is effected by this mechanism, in accordance to the results of Brost and Chatfield (1989).

The model does not include any explicit horizontal diffusion terms.

The model predicts the tracer concentration at the center of the grid cells. In order to compare model results to individual stations not located on grid cell centers horizontal and vertical interpolation has to be used. We interpolated in the horizontal direction the predicted concentration by means of two-dimensional Hermite cubics (de Boor, 1978) to the locations of the stations. In the vertical direction the concentration in the lowest model layer was selected as all station data available to the present study were obtained at ground level. This procedure neglects an explicit treatment of the boundary layer, which is justified if the tracer source is located remotely from the station under investigation. Furthermore, the Indian Ocean stations are located on relatively small islands which are not resolved on the model grid, but which induce some degree of vertical mixing due to their horizontal and vertical extent.

3. The simulation experiments

The simulation experiments were performed by running the model through 13 months, i.e., from the 1st of December 1978 through the entire wind data set of the GWE to the end of November 1979 and then again through the winds of December 1978. The first month of the simulation was considered as spin-up and discarded; all displayed results refer to the last 12 months of simulation. At every time step the source flux of ^{222}Rn is input at the lower boundary of the lowest model layer and the predicted atmospheric ^{222}Rn concentrations are corrected for the radioactive decay, using a mean lifetime of ^{222}Rn of 5.51 days.

3.1. Continental source of ^{222}Rn

The global average continental source flux of ^{222}Rn is estimated to lie between 0.75 and 1.2 atoms cm^{-2} s^{-1} (Lambert et al., 1982; Dörr, 1984). Little is known about regional differences of this source flux, but we estimate these differences relatively small when averaged over the large grid sizes of the transport model (500–1000 km). There exists few evidence of a relationship between the ^{222}Rn source flux and climatic parameters, such as surface air pressure, temperature or precipitation, which could be employed to establish a time dependence in the source flux. Indeed, Dörr (1984, p. 20ff) estimates that only variations in the barometric pressure might induce significant temporal variations in the ^{222}Rn source flux, which, however, do not exceed 50% on time scales of a few hours under extreme meteorological conditions. On the other hand, Dörr (1984) found that snowpack and freezing ground temperatures do reduce considerably the ^{222}Rn gas emanation rate from the soils.

Based on these considerations and because the region of interest in the present study is rather remote from local continental sources, we prescribed in all simulation experiments a ^{222}Rn source flux of 1 atom cm^{-2} s^{-1} distributed uniformly over the ice free continental areas. No temporal variations of this source flux were assumed in the model simulations, since most areas of the southern hemisphere continents except Antarctica do not exhibit sub-zero temperatures even in winter.

Several model experiments were also performed where we specified the land source of ^{222}Rn only on specific continents, such as Africa or South America, in order to examine the predicted relative contributions of each of the different continents to the combined atmospheric ^{222}Rn concentration burden at the monitoring sites under study.

3.2. Oceanic source of ^{222}Rn

The oceanic source flux of ^{222}Rn in general is two orders of magnitude smaller than the continental source flux (Wilkening, 1975; Peng et al., 1979). Nevertheless, in air masses which have not been in contact with continental surfaces for an appreciable time period, the concentration of ^{222}Rn will eventually decrease until a new equilibrium with the oceanic source is established. Indeed, it is believed, that a substantial fraction of the background levels (0.5–1.0 pCi m^{-3}) of ^{222}Rn measured at the Indian Ocean stations reflect oceanic origin (Polian et al., 1986). We performed a sensitivity simulation experiment which included an oceanic source term. Oceanic ^{222}Rn originates from the decay of ^{226}Ra in the surface layer of the ocean. A fraction of the generated ^{222}Rn escapes to the atmosphere. This flux, F_{sa}, is modeled by means of a bulk formula

$$F_{sa} = w_{ex}(C_s - \alpha_s P_a), \tag{1}$$

where C_s denotes the ^{222}Rn concentration in the ocean surface layer, α_s the solubility of radon in sea water and P_a the partial pressure of ^{222}Rn in the atmosphere. The exchange coefficient, w_{ex}, (often termed "piston velocity") is a function of the state of the sea surface. In the present study it was parameterized as a function of the 10 m wind speed according to the formulas given by Liss and Merlivat (1986) extended to include the effects of sea surface temperature and sea ice cover and scaled by a calibrating factor of 1.6 in analogy to the study by Heimann and Monfray (1989). The wind speeds needed to specify k_{ex} were obtained from the same GWE wind fields which were used in the transport model (see Section 2). Sea surface temperatures were prescribed from the monthly climatology of Levitus (1982) and ice cover was obtained from the data of Alexander and Mobley (1976).

The product $\alpha_s P_a$ occurring in (1) is in general much smaller than C_s, hence it was neglected in the computation of the oceanic source flux of ^{222}Rn.

The specification of the surface ocean concentration of ^{222}Rn, C_s, necessitates the solution of the balance equation for the ^{222}Rn concentration in the surface mixed layer:

$$\frac{d}{dt} hC_s = h(A_s - \lambda C_s) - F_{sa}, \tag{2}$$

where A_s denotes the oceanic activity of ^{226}Ra, λ the decay constant of ^{222}Rn ($\lambda^{-1} = 5.51$ days) and h the surface layer depth. Any oceanic horizontal or vertical convergence of ^{222}Rn is thereby neglected.

In the calculation we solved eq. (2) at every oceanic grid location of the model. The depth of

the surface layer, h, was held constant at 75 m. The activity of surface ocean ^{226}Ra was specified from GEOSECS data (Peng et al., 1979).

As an example Fig. 1b shows for a selected time period (July 1979) a time series of the calculated oceanic ^{222}Rn source flux at a specific location near Kerguelen (70°E, 49°S). The flux exhibits large variations, ranging from 0 to over 100 atoms m^{-2} s^{-1}. These variations are predominantly the result of changing surface wind speeds (shown in Fig. 1a). The deficit of the surface ocean ^{222}Rn reservoir relative to an equilibrium with the oceanic ^{226}Ra concentration is also illustrated in Fig. 1a. It is changing between 15 and 35%.

4. Observational data

^{222}Rn data from 4 remote monitoring stations in the southern Indian Ocean and on the Antarctic coast have been used in the present study. The geographic locations of these stations are given in Table 1. All stations have been in operation since 1960. An in-depth description of the sampling techniques and the data analysis procedures used has been given by Polian (1984) and Polian et al. (1986).

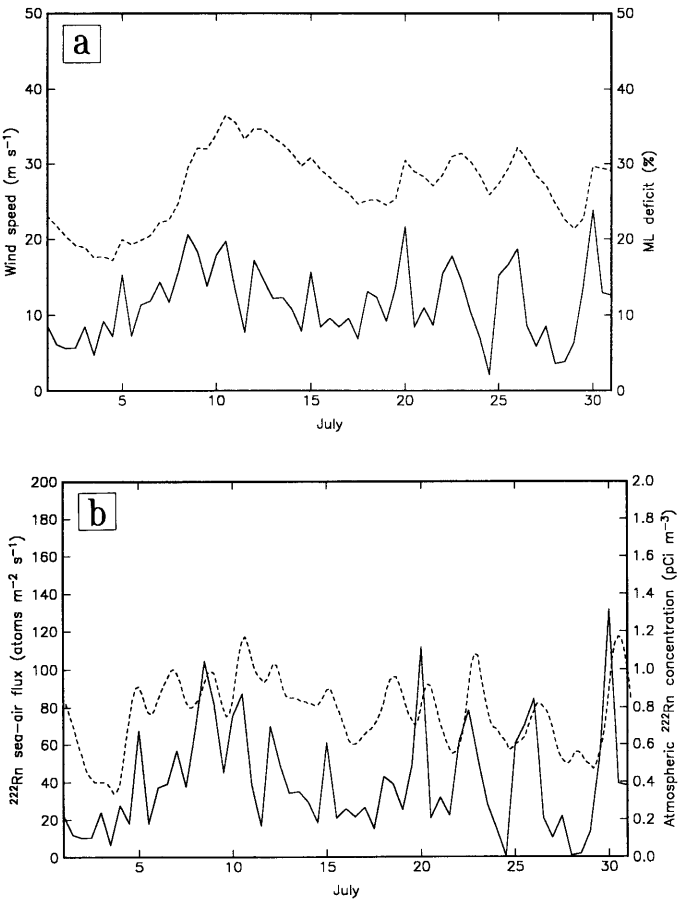

Fig. 1. (a) Solid line: Time series of surface wind speed as recorded in the GWE dataset in the vicinity of Kerguelen (70°E, 49°S) during July 1979. Dashed line: Calculated sea surface ^{222}Rn concentration deficit expressed in % relative to equilibrium with oceanic ^{226}Ra. (b) Solid line: Time series of calculated sea–air source flux of ^{222}Rn. Dashed line: Calculated atmospheric ^{222}Rn concentration at the same location based on only the oceanic ^{222}Rn source component (see text).

Table 1. *Locations of ^{222}Rn monitoring stations*

Crozet Island	51°E 46°S
Amsterdam Island	77°E 37°S
Kerguelen	70°E 49°S
Dumont d'Urvllle	140°E 66°S

4.1. Sampling method

The air sampling system is designed to quantify the radioactivity of the daughter elements of ^{222}Rn with short life-times: ^{218}Po, ^{214}Pb and ^{214}Bi. These decay products, after formation being rapidly attached to aerosols, are accumulated for 2 h on a filter by means of an airpump. Every 2 h the filter is replaced. Subsequently the filter activity is determined by measurements during the 2 h following the sampling. The detection efficiency is calibrated by means of standard filters measured in the laboratory. The half lives of the three ^{222}Rn daughter elements are shorter than 30 min. The measurement method assumes that ^{222}Rn in the sampled air is in equilibrium with its three daughter elements. We thus neglect the problem of aerosol wash-out by rainfall. The precision ($1\ \sigma$) of the individual measurement is 10% at a concentration level of 1 pCi m^{-3}; due to the counting statistics it varies inversely proportional to the square root of the concentration. The detection limit is estimated at 0.01 pCi m^{-3}.

4.2. Data selection

For all the comparisons to the model experiments only data records from the GWE period December 1978 through November 1979 were chosen. These data were subsequently screened to remove time intervals during which, because of low wind speeds, locally emanated ^{222}Rn may mask the ^{222}Rn advected from remote continents. This local contamination was excluded based on another trace gas, ^{220}Rn, which is produced in the soil similar to ^{222}Rn. Since the half-life of ^{220}Rn is only 54 s and that of its solid daughter element, ^{212}Pb, is 10.6 h it therefore cannot reach in general the Indian Ocean islands from continental areas in view of transit times exceeding a few days.

In practice, we excluded all data of time intervals during which the concentration of ^{220}Rn exceeded 0.1 pCi m^{-3}. At Crozet Island, this threshold level was increased by a factor of two in order to take into account the relative proximity of the South African continent (2400 km) from which, during periods of strong winds, a non-negligible amount of ^{220}Rn may be advected. This selection criterion resulted at Crozet and Amsterdam Islands, and at the Antarctic coast in the exclusion of only a few percent of the total sampling time. At Kerguelen, because of the large size of the island, almost 20% of the data, mostly during summer, had to be excluded. Finally, the data with a time resolution of 2 h were converted to the computational time resolution of the model (4 h) by smoothing the original values by means of a filter with weights (0.25, 0.5, 0.25).

5. Discussion of results

The results of the simulation study are presented in the following order. Firstly, we describe how the model renders the synoptic time scale variations of the ^{222}Rn concentration. Then we discuss the annual cycle and mean annual ^{222}Rn concentration level at the monitoring stations. All the model results refer to simulation runs using only the continental source unless stated otherwise. The discussion of the oceanic contribution to the tropospheric concentration of ^{222}Rn is deferred to the final subsection below.

5.1. Synoptic time scale

5.1.1. Radon storms. Most spectacular in the observed time series of the ^{222}Rn concentration at the Indian Ocean monitoring stations are the so-called "radon storms", short time intervals (6–12 h) during which the ^{222}Rn concentration rises by a factor of 5 or more. Polian et al. (1986) have shown by means of trajectory analyses how such events are associated with the passage of synoptic scale disturbances which, a few days before, had moved over the South African continent.

Figs. 2a–f show in detail how such an event is simulated in the transport model. Displayed are predicted instantaneous ^{222}Rn concentration fields in the lowest model layer over the southern Atlantic and Indian Ocean on 6 consecutive days

at 00 GMT from 4 July to 9 July, 1979. Also shown are contour lines of the geopotential height of the 850 hPa surface.

The strong concentration contrast between continental and oceanic air masses is clearly seen. The sequence of frames in Fig. 2 shows how the depression located on 4 July south of the tip of Africa draws at its northern flank ^{222}Rn enriched air off the continent out over the ocean. By 6 July the ^{222}Rn plume extends all the way through 70°E, resulting in a marked concentration increase at the Indian Ocean stations. On the subsequent days the plume broadens and concentration values decrease due to radioactive decay and vertical and horizontal mixing. By 9 July the same ^{222}Rn enriched air mass is located at 100°E, being partially detached from the African source region.

On 8 July, a further ^{222}Rn plume is seen to enter the Indian Ocean area (60°S, 20°E), representing an air mass originating over South America. It is associated with a second cyclone centered at 70°S, 10°W. One day later it has moved to 40°E and is being advected by strong south-westerly winds toward Kerguelen.

The vertical structure of the concentration fields on 9 July is displayed in three zonal cross sections located at 43°, 51° and 59°S in Fig. 3 and in a meridional cross section at 60°E in Fig. 4. In the zonal cross sections both ^{222}Rn plumes referred to above are seen to be slanted towards the East with height resulting from higher wind speeds aloft. The South American plume is also slanted toward the north and exhibits maximal concentrations at mid-troposphere levels. These modeled events demonstrate the possibility of higher ^{222}Rn concentrations aloft than at sea level, such as have been observed in vertical profiles obtained over Kerguelen (Polian et al., 1986).

5.1.2. Comparison with station data. Fig. 5 shows modeled and observed time series of the ^{222}Rn concentration at the three Indian Ocean stations for the month of July 1979. The radon event discussed in the previous subsection is seen as large peaks occurring on 6–7 July at the three locations.

There is a fair correspondence between model and data as to the time of occurrence of individual ^{222}Rn events; however, amplitude and width of the ^{222}Rn peaks differ considerably between model prediction and data. Furthermore, the model predicts at all stations a too high background concentration level.

The model is seen to result in too diffuse ^{222}Rn peaks: e.g., at Crozet Island the model predicts a single event occurring between 4 July through 7 July, which in reality is recorded in the data as two separate peaks on 4 July and on 6 July. This general model behaviour is summarized in Fig. 6, displaying at the three Indian Ocean stations the autocorrelation functions (ACF) of both time series, model and data. These ACFs were calculated from the entire year of simulation. The too diffusive character of the model generated time series is evident: the lag at which the ACF drops below 0.5 is twice as large as in the ACF of the data time series.

Several model deficiencies contribute to this result. Evidently, the poor horizontal resolution of the model limits the achievable time resolution. Indeed, at the latitudes of the stations the model grid cells extend zonally over about 500 km; requiring more than 7 h to traverse at wind speeds of typically 20 m s^{-1}. Also, the meteorological data used by the model to calculate advective transport have a time resolution of 12 h. Furthermore, the distance between the Indian Ocean islands and the nearest continental source region is only about 3 to 6 grid cells, which is hardly sufficient to resolve faithfully the steep concentration gradient of ^{222}Rn in the lower model levels between continental and maritime regions. In order to assess the rôle of the numerical advection scheme we performed a sensitivity experiment using a scheme conserving second order moments of the tracer distribution described by Prather (1986). This experiment, however, resulted only in a minor improvement compared to the results obtained with the standard slopes scheme of Russel and Lerner (1981). The influence of model resolution on the predicted horizontal concentration fields may be further appreciated by comparing Fig. 2 with the model results of Balkanski and Jacob (1990, Fig. 6). The effects of the higher resolution (a factor of two in both horizontal directions) in conjunction with Prather's (1986) advection scheme is not readily apparent. We thus speculate that only a model with even finer resolution might render realistically the fine structure of the observed ^{222}Rn concentration records.

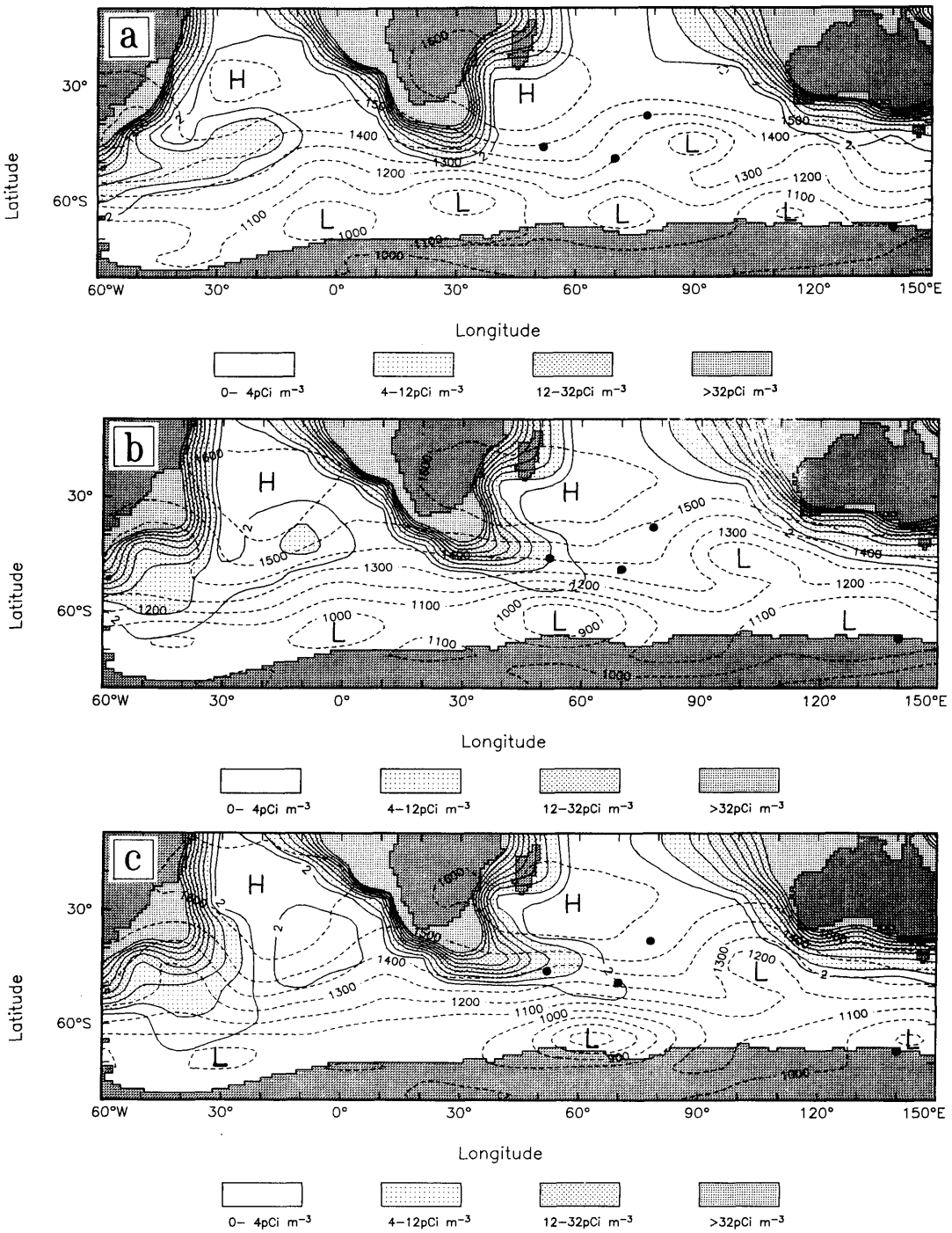

Fig. 2. Model simulation of a "radon storm" over the Southern Atlantic and Indian Ocean 4 July–9 July 1979. Each panel (a–f) depicts concentration of ^{222}Rn in the surface model layer (solid contour lines, contour interval: 2 pCi m^{-3} below a level of 4 pCi m^{-3} and 4 pCi m^{-3} in the range from 4 to 32 pCi m^{-3}; concentration levels above

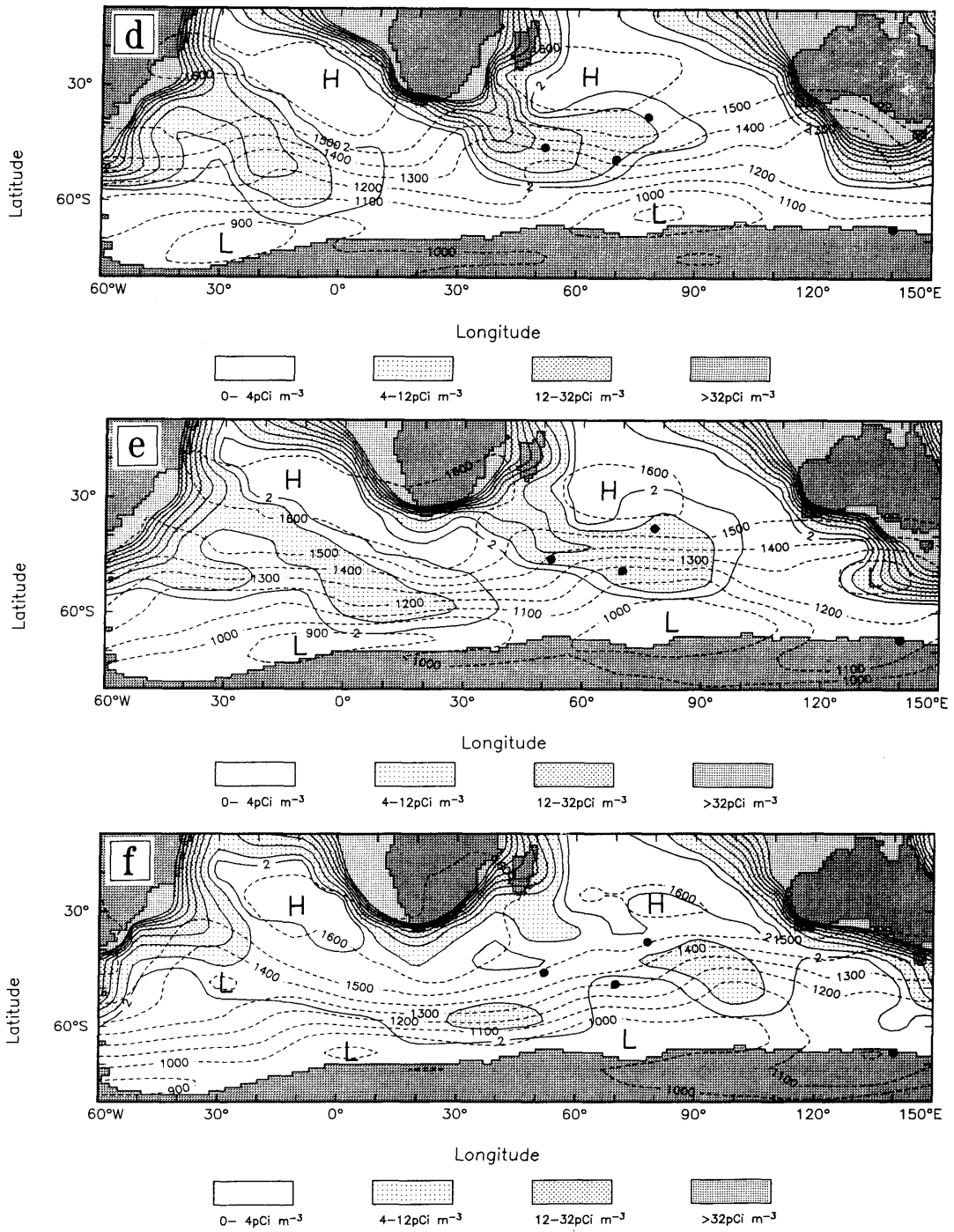

4 pCi m^{-3} are stippled) and height of the 850 hPa pressure surface (dashed contour lines, contour interval: 100 gpm) at 00 GMT on consecutive days. Letters mark the centers of major Highs (H) and Lows (L), respectively. Black circles indicate locations of the monitoring stations listed in Table 1.

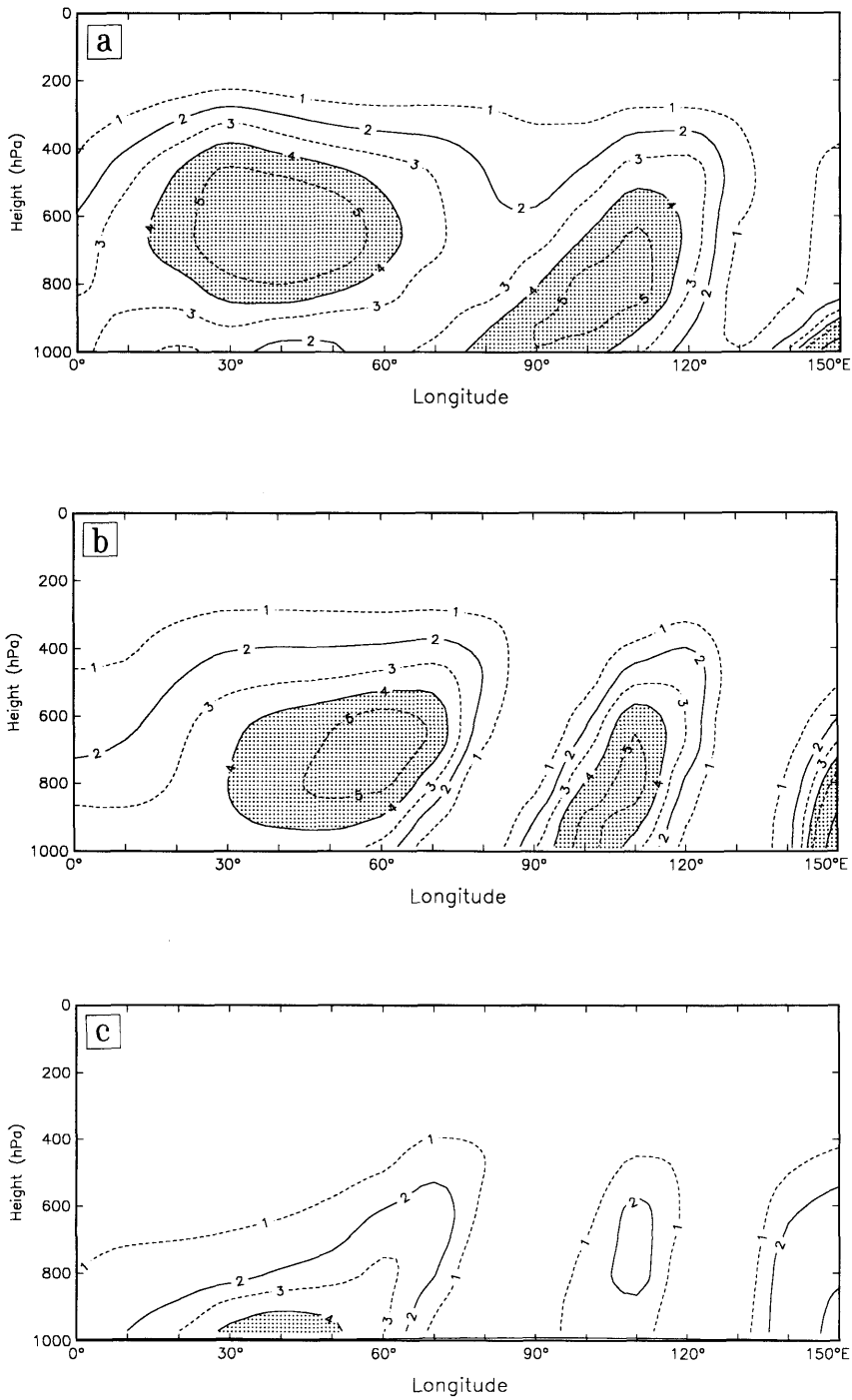

Fig. 3. Simulated zonal-height cross sections of ^{222}Rn concentration on 9 July 1979, 00 GMT at 43° (a). 51° (b) and 59°S (c). Contour interval is 1 pCi m^{-3}; stippled areas indicate concentrations above 4 pCi m^{-3}.

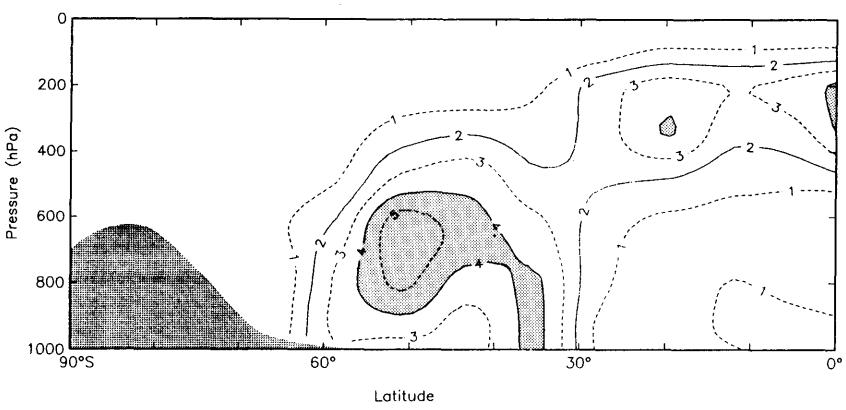

Fig. 4. Simulated meridional-height cross section of ^{222}Rn concentration at 60°E on 9 July 1979, 00 GMT. Contour interval is 1 pCi m^{-3}; stippled areas indicate concentrations above 4 pCi m^{-3}.

Also shown in Fig. 6 are the cross-correlation functions (CCF) between the model and data time series. At all three stations the CCF exhibits a significant correlation (>99.9%, the significance levels were calculated taking into account the reduction of the degrees of freedom due to the autocorrelation in the model and the data time series) at lag 0, thus confirming the synchrony between the time series.

A further comparison between model and data is provided for in Fig. 7 showing the CCF between the time series of Crozet Island and Kerguelen in the model and as observed. Both curves exhibit a distinct maximal correlation, the signal at Crozet Island leading by 20 h in the simulation and by 16 h in the data. In view of the model limitations discussed above, the difference between these two lag times is not significant. This lag represents a typical transit time for a ^{222}Rn event to traverse the distance between the two stations (approximately 1400 km). It corresponds to an average advection velocity of the order of 20 m s^{-1}. Similar lag times have been reported by Polian et al. (1986).

A further manifestation of the too diffusive character of the model generated concentration fields is provided for in Fig. 7b, where the CCF between model and data time series of Kerguelen and Amsterdam Island are displayed. Here the model exhibits a significant correlation, Kerguelen leading by 20 h. But the observed time series are uncorrelated, the reason being that Amsterdam Island, although lying only about 1400 km to the north of Kerguelen, experiences quite a different climate than the latter. In the model they are separated by only one and a half grid cells which is not sufficient to effectively distinguish between the two stations.

5.2. Annual cycle

A summary of the comparison between model predictions and observations is provided for in Fig. 8, showing the annual cycle of the monthly mean ^{222}Rn concentration at the locations of the four monitoring stations for the 12 months where windfields were available. Table 2 lists the observed and model predicted mean annual concentration levels. We also include the predicted concentration levels at the Antarctic coast stations Mawson and G. v. Neumaier where currently ^{222}Rn is also measured.

5.2.1. Mean annual concentration levels. A major discrepancy between model and data is readily apparent in Fig. 8. The model seriously overestimates the annual mean ^{222}Rn concentration levels. Table 2 shows that the overestimation exceeds a factor of two at Crozet Island and at Kerguelen, it is still larger than 1.6 at Amsterdam Island. Only at the Antarctic coast station does the model predict a mean concentration level in accordance with the observations.

Table 2 lists also at the stations the contribution to the mean annual ^{222}Rn level calculated from the model experiment using the oceanic source only. If this signal were added to the continental contribution the discrepancy between

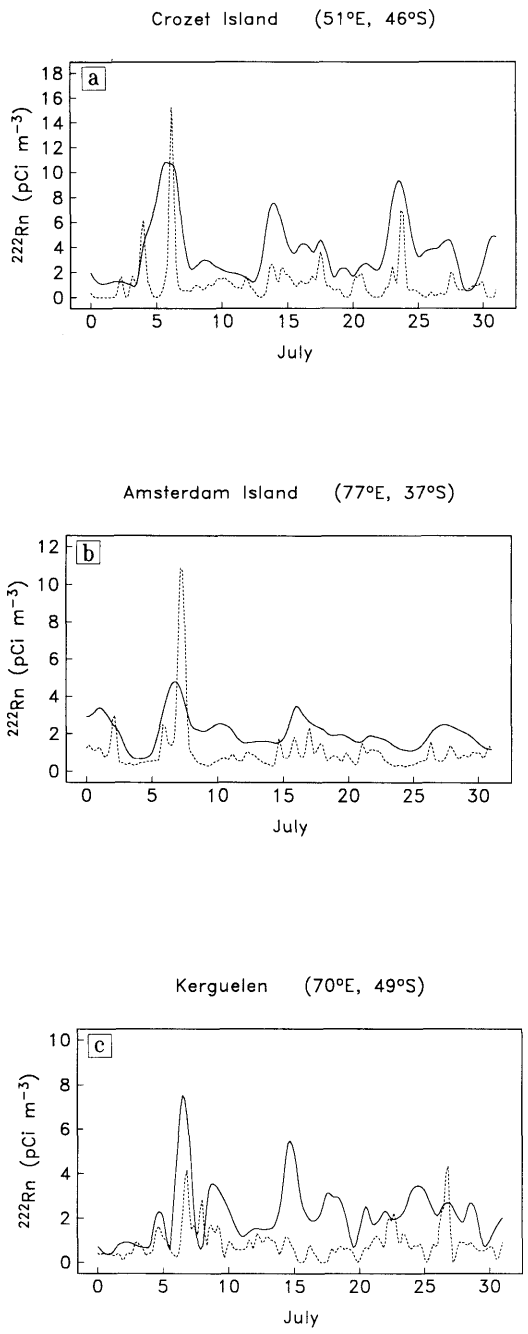

Fig. 5. Time series of simulated (solid lines) and observed (dashed lines) ^{222}Rn concentration at the Indian Ocean monitoring stations for the month of July 1979. (a) Crozet Island, (b) Amsterdam Island, (c) Kerguelen.

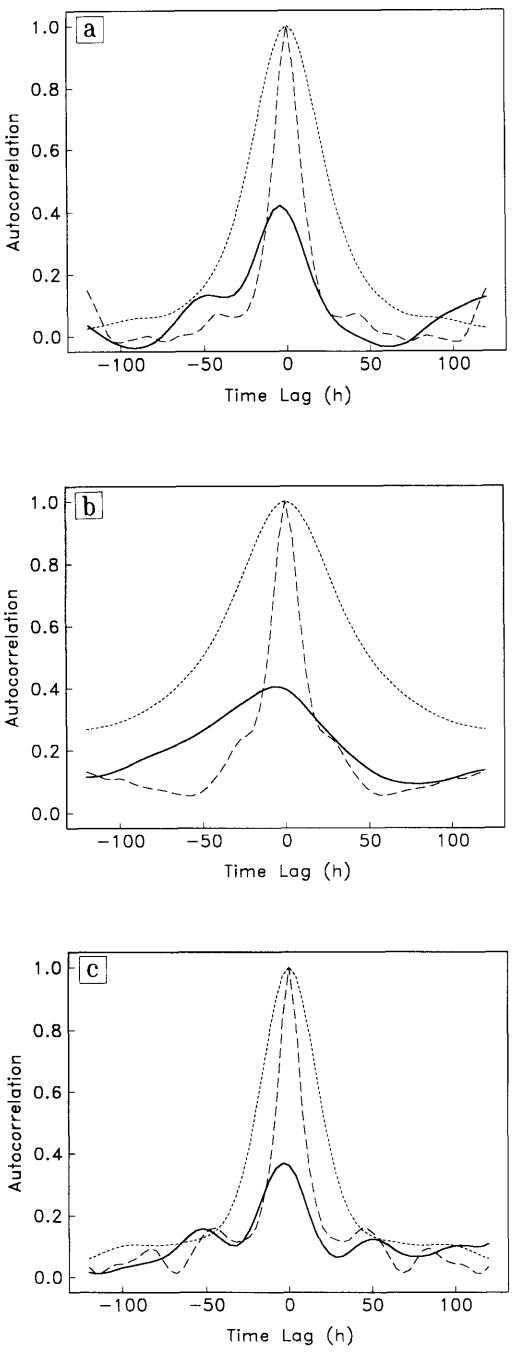

Fig. 6. Autocorrelation functions of data (long dashes), model simulation (short dashes) and cross-correlation functions between model and data (solid lines) at (a) Crozet Island, (b) Amsterdam Island, (c) Kerguelen.

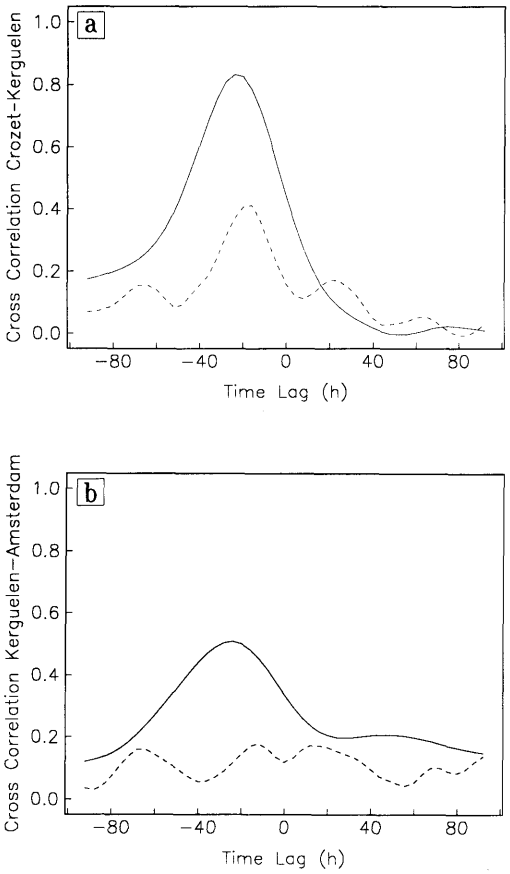

Fig. 7. Cross-correlation functions between time series at Crozet and Kerguelen (a) and between Kerguelen and Amsterdam Island (b). Solid line: model, dashed line: observations.

model simulation and data would be even larger. Three principal sources of error may contribute to this result:

(1) The continental source strength of ^{222}Rn was set arbitarily at 1 atom cm^{-2} s^{-1} in the simulation experiments. This value is uncertain to almost a factor of two; but we hesitate to attribute the entire discrepancy apparent in the present simulation to this single reason.

(2) A further source of error may be insufficient vertical exchange between lower and upper model layers over the South African source region. If this were the case it would lead to too high concentrations over the continent in the air masses of lowermost model layers which subsequently are advected over the oceans. In principle this possibility could be checked if ^{222}Rn measurements in the close proximity of South Africa were available. Brost and Chatfield (1989) find in their model experiments a strong dependency of predicted marine surface concentrations as a function of the strength of the vertical subgrid scale parameterization. In particular they obtain the lowest concentrations in remote marine areas when selecting the strongest cloud transport scheme at their disposal.

(3) Finally the coarse resolution of the present model might also contribute to the disagreement model and data, in particular at Crozet Island lying only three grid cells off the coast of Africa. As already noted above in Subsection 5.1.2 this is insufficient to fully resolve the steep concentration gradient which develops between continent and oceans in the lowermost model layers

Table 2. *Predicted and observed mean annual concentration (in pCi m^{-3}) of ^{222}Rn at the monitoring stations*

		Model	
Location	Observations	Continenal source	Oceanic source
Crozet Island	1.02	2.56	0.86
Amsterdam Island	0.84	1.35	0.59
Kerguelen	0.79	1.58	1.01
Dumont d'Urvlle	0.77	0.70	0.42
G. v. Neumaier (8°W, 70°S)	—	0.61	0.24
Mawson (63°E, 67°S)	—	0.45	0.35

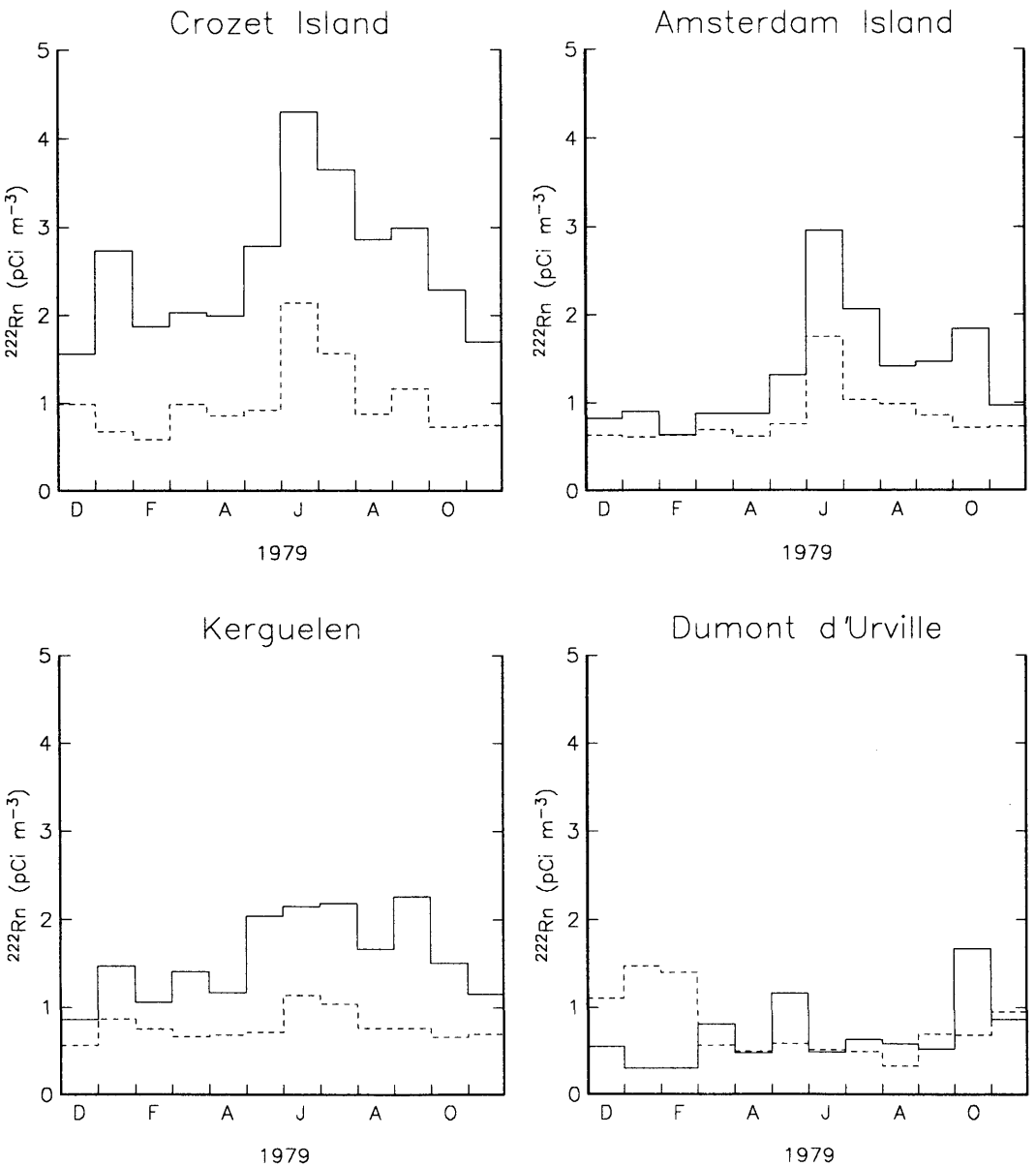

Fig. 8. Observed (dashed line) and model predicted (solid line) monthly mean concentration of ^{222}Rn at the monitoring stations in the Indian Ocean and at the Antarctic coast during December 1978 to November 1979.

(see Fig. 2 above). Indeed, Balkanski and Jacob (1990), using a model with twice the horizontal resolution in latitudinal and zonal direction than employed here, do not experience this problem of too high annual mean concentration levels.

5.2.2. The annual cycle at the Indian Ocean stations. The atmospheric concentration of ^{222}Rn at the Indian Ocean stations exhibits a distinct annual cycle, with highest concentration during the winter months, when the subtropical highs in

the southern hemisphere are displaced towards the north and consequently cyclonic disturbances frequently can pass over southern Africa thereby picking up continental ^{222}Rn which is subsequently advected over the Indian Ocean (Polian et al., 1986). In the summer season the wind regimes generally are displaced southwards. The subtropical highs now effectively block the South African source region from being reached by midlatitude cyclones. Consequently at the Indian Ocean islands the ^{222}Rn concentration remains at low background levels.

This particular feature is well represented in the model simulation, both in phase and in amplitude at the Indian Ocean stations.

5.2.3. The annual cycle at the Antarctic Coast. At the Antarctic coast the observed annual cycle of ^{222}Rn exhibits a phase opposite to the cycle at the midlatitude stations further to the north. Here maximal ^{222}Rn concentrations are found in southern hemisphere summer. The primary mechanism establishing this peculiar phase is not evident. Based on a few vertical profiles taken in the lower troposphere over the Antarctic coast and on other tracers besides ^{222}Rn, Polian et al. (1986) conjecture that the enhanced levels in summer reflect air masses originating from the midlatitude southern hemisphere continents carried aloft by convective processes and subsequently transported in the middle and upper troposphere toward the Antarctic continent.

As seen in Fig. 8 the model simulation fails entirely to reproduce the phase at the Antarctic coast station Dumont d'Urville. Furthermore no significant correlation is found between model predicted and observed time series at this station. We attribute this apparent discrepancy to pecularities of the Dumont d'Urville station, which are not properly accounted for in the transport model. Often during winter a shallow inversion layer forms which cuts off the station from the overlying free troposphere. This layer is fed by cold air descending from the Antarctic ice sheet. The locally measured concentration of ^{222}Rn therefore may drop to very low values. This specific boundary layer structure is not resolved in the model; the simulated winter concentration at Dumont d'Urville thus is more representative of the free troposphere at that latitude.

During the summer season, this explanation can not hold. Here, the model predicts only a few synoptic scale ^{222}Rn events with small amplitudes but the observations show much larger concentration peaks. Again no significant correlation between model and data is found. We may speculate that the quality of the GWE wind fields in the Antarctic regions is not sufficient for the present purpose.

5.2.4. Contributions due to individual continents. Table 3 lists the relative contributions of each of the southern hemisphere continents to the predicted total ^{222}Rn concentration burden at the monitoring stations. As expected ^{222}Rn emanating off the African continent at all Indian Ocean stations constitutes a sizeable contribution. More surprising, however, is the result that all three stations are also significantly influenced by ^{222}Rn from the South American continent. A direct verification of this model result is difficult to provide, however, the maps shown in Subsection 5.1 (Fig. 2) document a particular case of a model predicted air mass carrying ^{222}Rn from South America to the Indian Ocean stations. Table 3

Table 3. *Relative contribution (in %) of the southern hemisphere continents to the total model predicted ^{222}Rn concentration at several monitoring stations*

Station location	Africa	South America	Australia and NZ
Crozet Island	60	37	3
Amsterdam Island	53	45	2
Kerguelen	48	49	3
Dumont d'Urville	14	20	67
G. v. Neumaier	2	87	11
Mawson	27	64	9

also lists the partitioning at three Antarctic coast stations. Each is influenced primarily by its nearest southern hemisphere continent. In view of the model's limited realism close to Antarctica these results, however, must be considered as preliminary.

5.3. *Concentration signal of oceanic ^{222}Rn*

The sensitivity simulation experiment involving the oceanic source of ^{222}Rn resulted in mean annual concentration levels at the stations as listed in Table 2. The predicted signal of oceanic ^{222}Rn is quite variable (see Fig. 1b for an example) but it does not exhibit the distinct peaks of high concentrations which are characteristic of continental ^{222}Rn. Also we do not find any distinct seasonal variation in the predicted oceanic ^{222}Rn concentration signal.

The simulation results in quite realistic background ^{222}Rn concentrations levels from the oceanic source alone. However, in the present model continental ^{222}Rn already induces background levels which mask the oceanic signal entirely. Indeed, adding the oceanic to the continental signal does not improve any of the correlations between observations and simulation. Only if the model generated concentration fields were less diffuse in time and space then the oceanic signal might be detectable during periods not influenced by continental air masses.

6. Conclusions

The simulations of the long-range transport of ^{222}Rn over the Indian Ocean carried out with the present three-dimensional model are far from perfect. Although significant correlations are found between model prediction and observations at the Indian Ocean monitoring stations, there nevertheless remain discrepancies which have to be adressed in future modeling efforts. The lack of agreement at Dumont d'Urville indicates that the tropospheric transport pathways from the southern hemisphere continents to the Antarctic coast have not been properly accounted for in the model. This is of particular importance for the interpretation of trace elements recorded in Antarctic ice.

Obviously, a considerable effort in improving the transport model has to be invested in order to obtain a better agreement between simulation and data. The most promising areas of model developments include the parameterization of subgrid-scale convection, representation of the planetary boundary layer and increasing the horizontal resolution. A further improvement might be achieved by means of a superior numerical advection scheme, as the present simulations appear to result in too diffusive tracer concentrations.

The quality of the available meteorological fields constitutes an essential limitation to the present modeling approach. In data sparse areas, such as the region under study, the meteorological analyses depend almost entirely on the quality of the operational weather forecast models used in the assimilation scheme. These have improved considerably during the last decade, hence we may expect a better performance of the transport model if driven by wind fields from a more recent period than the GWE.

Nevertheless, our simulation experiments demonstrate that the presently available Indian Ocean ^{222}Rn data provide a powerful test of a transport model. The ^{222}Rn concentration fields as calculated with the model exhibit considerable spatial structures also in the vertical dimension, which might be tested if vertical profiles were available. The fact that the present model is driven essentially by observed winds constitutes a distinct advantage, as it permits a direct comparison between model simulation and data on a day to day base.

7. Acknowledgement

P. M. was supported by the Commission of the European Communities' climatology and natural hazards program (contract no. EV4C-0030-D(B)). This is a revised version of Report No. 32 of the Max-Planck-Institute für Meteorologie and constitutes contribution No. 1032 of the Centre des Faibles Radioactivités.

REFERENCES

Alexander, R. C. and Mobley, R. L. 1976. Monthly average sea surface temperatures and ice pack limits on a 1 deg global grid. *Mon. Weather Rev. 104*, 143–148.

Bengtsson L., Kanamitsu, M., Kållberg, P. and Uppala, S. 1982. FGGE 4-dimensional data assimilation at ECMWF. *Bull. Am. Meteorol. Soc. 63*, 29–43.

Brost, R. A. and Chatfield, R. B. 1989. Transport of radon in a three-dimensional, subhemispheric model. *J. Geophys. Res. 94*, 5095–5119.

de Boor, C. 1978. *A practical guide to splines.* New York: Springer, 392 pp.

Dörr, H. 1984. Investigation of the gas- and water-balance in the unsaturated soil zone by means of measurements of carbon dioxide and ^{222}Rn (in German). Thesis, University of Heidelberg, FRG.

Dörr. H. and Münnich, K. O. 1987. Annual variation in soil respiration in selected areas of the temperate zone. *Tellus 39B*, 114–121.

Dörr, H., Kromer, B., Levin, I., Münnich, K. O. and Volpp, H.-J. 1983. CO_2 and ^{222}Rn as tracers for atmospheric transport. *J. Geophys. Res. 88*, 1309–1313.

Fung, I., Prentice, K., Matthews, E., Lerner, J. and Russell, G. 1983. Three-dimensional tracer model study of atmospheric CO_2: Response to seasonal exchanges with the terrestrial biosphere. *J. Geophys. Res. 86*, 1281–1294.

Hansen, J., Russell, G., Rind, D., Stone, P., Lacis, A., Lebedeff, S., Ruedy, R. and Travis, L. 1983. Efficient three-dimensional global models for climate studies: Models I and II. *Mon. Wea. Rev. 111*, 609–662.

Heimann, M. and Keeling, C. D. 1989. *A three-dimensional transport model for atmospheric CO_2: 2. Model description and simulated tracer experiments.* Report No. 33, Hamburg: Max-Planck-Institute für Meteorologie, 105 pp.

Heimann, M., and Monfray, P. 1989. *Temporal and spatial variations of the gas exchange coefficient for CO_2: Data analysis and global validation.* Report No. 31, Hamburg: Max-Planck-Institute für Meteorologie, 29 pp.

Heimann, M., Keeling, C. D. and Fung, I. Y. 1986. Simulating the atmospheric carbon dioxide distribution with a three-dimensional tracer model. In: *The changing carbon cycle: a global analysis* (eds. J. R. Trabalka and D. E. Reichle). New York: Springer-Verlag, 16–49.

Jacob, D. J., Prather, M. J., Wofsy, S. C. and McElroy, M. B. 1987. Atmospheric distribution of ^{85}Kr simulated with a general circulation model. *J. Geophys. Res. 92*, 6614–6626.

Lambert, G., Polian, G., Sanak, J., Ardouin, B., Buisson, A., Jegou, A. and Le Roulley, J. C. 1982. The cycle of radon and of its daughter products: Application to the investigation of troposphere-stratosphere exchanges (in French). *Ann. Geophys. 38*, 497–531.

Levitus, S. 1982. *Climatological atlas of the world ocean.* NOAA professional paper 13, Rockville, 173 pp.

Liss, P.S. and Merlivat, L. 1986. Air–sea gas exchange rates: Introduction and synthesis. In: *The Rôle of Air–Sea Exchange in Geochemical Cycling* (ed. P. Buat-Ménard). Dordrecht/Holland: Reidel, 113–127.

Liu, S. C., McAfee, J. R. and Cicerone, R. J. 1984. Radon-222 and tropospheric vertical transport. *J. Geophys. Res. 89*, 7291–7297.

Peng, T.-H., Broecker, W. S., Mathieu, G. C. and Li, Y.-H. 1979. Radon evasion rates in the Atlantic and Pacific oceans as determined during the Geosecs program. *J. Geophys. Res. 84*, 2471–2486.

Polian, G. 1984. *Atmospheric transport in the Southern Hemisphere and the global balance of ^{222}Rn* (in French). Thesis, Paris/France: Université Pierre et Marie Curie, 227 pp.

Polian, G., Lambert, G., Ardouin, B. and Jegou, A. 1986. Long-range transport of continental radon in subantarctic and antarctic areas. *Tellus 38B*, 178–189.

Prather, M. J. 1986. Numerical advection by conservation of second-order moments. *J. Geophys. Res. 91*, 6671–6681.

Prather, M. J., McElroy, M. B. Wofsy, S. C. Russell, G. and Rind, D. 1987. Chemistry of the global troposphere: fluorocarbons as tracers of air motion. *J. Geophys. Res. 91*, 6671–6681.

Russell, G. L. and Lerner, J. A. 1981. A new finite-differencing scheme for the tracer transport equation. *J. Appl. Meteor. 20*, 1483–1498.

Wilkening, M. H. and Clements, W. E. 1975. Radon-222 from the ocean surface. *J. Geophys. Res. 80*, 3828–3830.